Kinetic Theory of Transit Time Magnetic Pumping and Alfvèn Wave Heating

Satish Puri

IPP 4/183 November 1979

MAX-PLANCK-INSTITUT FÜR PLASMAPHYSIK

8046 GARCHING BEI MÜNCHEN

MAX-PLANCK-INSTITUT FÜR PLASMAPHYSIK

GARCHING BEI MÜNCHEN

Kinetic Theory of Transit Time Magnetic Pumping and Alfvèn Wave Heating

Satish Puri

IPP 4/183 November 1979

Die nachstehende Arbeit wurde im Rahmen des Vertrages zwischen dem Max-Planck-Institut für Plasmaphysik und der Europäischen Atomgemeinschaft über die Zusammenarbeit auf dem Gebiete der Plasmaphysik durchgeführt.

KINETIC THEORY OF TRANSIT TIME MAGNETIC PUMPING AND ALFVÈN WAVE HEATING

Satish Puri

Max-Planck-Institut fuer Plasmaphysik,

EURATOM-Association, D-8046 Garching

ABSTRACT

Coupling, conversion (from primarily compressional to a mixed torsional/compressional character near the critical Alfvèn surface), and absorption of Alfvèn waves in a hot, inhomogeneous plasma is studied using idealized current carrying antennas. Only an insignificant fraction of the energy coupled by the antenna into the compressional wave is delivered to the plasma either by wave conversion or through direct transit time attenuation of the compressional wave.

Previous attempts at studying the Alfvèn wave heating of a plasma have employed either the MHD[1,2] or a mixed MHD and kinetic[3,4] description of the plasma. Hasegawa and Chen[3] pioneered the existence of the kinetic Alfvèn wave (KAW) which is the hot-plasma counterpart of the torsional Alfvèn wave if the electron thermal velocity, v_z, exceeds the phase velocity, v_p, of the wave along the direction of the static magnetic field B_o. Unlike the torsional Alfvèn wave, the KAW propagates on the high density side of the Alfvèn surface (where $v_p = v_A$, the local Alfvèn speed); this opens up the possibility of heating the interior of a plasma by the electron Landau damping (ELD) of this wave which is excited through the wave conversion of the evanescent compressional Alfvèn wave (CAW) launched by a current carrying antenna located outside the plasma boundary. Stix[5] has pointed out that only a part of the CAW will convert into the KAW,

the rest being transmitted further across the Alfvèn surface as a propagating CAW. The object of this paper is to obtain a quantitative dilineation of the fractional energy coupled respectively into the propagating KAW and CAW across the Alfvèn layer by the evanescent CAW launched by the antenna.

Figure 1 shows a semi-infinite maxwellian plasma slab unform in the y and z directions and with a linear density profile, immersed in a magnetic field B_0 along the z direction. The ideal antenna at x = -b carries a unit current $J_y = \exp(i\, k_z z)$.

The Alfvèn wave dispersion characteristics for a hot plasma are shown in Fig. 2. At the cutoffs x_{c1} and x_{c2}, the evanescent CAW and KAW change into propagating KAW and CAW, respectively. Between the antenna and the Alfvèn surface x_A, the KAW, principally a torsional wave with the field components E_x, E_z and H_y, is so strongly evanescent that an attempt to launch it directly from the antenna would be futile. This explains the antenna configuration for launching the CAW (with field components E_y, H_x and H_z), which is only weakly evanescent between the antenna and the Alfvèn surface. It will be presently shown that CAW is essentially undamped and real hope in heating the plasma consists in an efficient conversion to the KAW in the region of the Alfvèn layer.

For CAW, the wavelength component $\lambda_x >> r_{ci}$, the ion gyroradius everywhere in the plasma slab. Also, in the critical region near x_A, where significant coupling and energy transfer from CAW to KAW might be expected, $\lambda_x >> r_{ci}$ for KAW as well. The energy coupled to KAW is rapidly absorbed through ELD in a short distance along the x-direction and the accuracy of the dispersion characteristics outside the critical region will not reflect on our results where we are primarily interested in determining the extent

to which the energy launched by the antenna is converted to and thereby absorbed by the KAW. Consequently, in the present context, it would suffice to retain only the zeroeth order terms in r_{ci}/λ_x in the dielectric tensor elements, i.e. the plasma may be considered cold in the perpendicular direction. This simplification allows us to treat the plasma as "locally homogeneous".

With these provisions, the "local" dispersion relation may be written in the form

$$A n_x^4 - B n_x^2 + C = 0, \tag{1}$$

where $A = \epsilon_x$, $B = \epsilon_x^2 + \epsilon_y^2 + \epsilon_x \epsilon_z - \epsilon_x n_z^2 - \epsilon_z n_z^2$, $C = \epsilon_z (\epsilon_x^2 + \epsilon_y^2 - 2\epsilon_x n_z^2 + n_z^4)$, $n_z = ck_z/\omega$, $k_z = 2\pi/\lambda_z$,

$$\epsilon_x \simeq 1 - \Sigma \left[\omega_{pj}^2 / (\omega^2 - \omega_{cj}^2) \right], \tag{2}$$

$$\epsilon_y \simeq -i \Sigma s_j (\omega_{cj}/\omega) \left[\omega_{pj}^2 / (\omega^2 - \omega_{cj}^2) \right], \tag{3}$$

$$\epsilon_z \simeq 1 - \Sigma (\omega_{pj}^2 / \omega^2) \varsigma_j^2 Z_j'(\varsigma_j), \tag{4}$$

s_j is the sign of the charge of the particle, $\varsigma_j = c/n_z v_{zj}$, Z_j is the plasma dispersion function[6], $Z'_j = \partial Z_j / \partial \varsigma_j$ while the summations are to performed over all the particle species. In this paper we treat an equal mixture of fully ionized deuterium and tritium throughout.

The left and right coutoffs at x_{c1} and x_{c2} occur for C = 0 in (1) and are located by $n_z^2 = \epsilon_x \mp i \epsilon_y$. Equation (1) may be factored into quasi-compressional and quasi-torsional roots, respectively, as

$$n_x^2 = \epsilon_x - n_z^2 + \delta_1 , \tag{5}$$

and $$n_x^2 = (\epsilon_z/\epsilon_x)(\epsilon_x - n_z^2) + \delta_2 \tag{6}$$

where $$\delta_1 = [q - (q^2 - 4pr)^{1/2}]/2p , \tag{7}$$

$p = \epsilon_x$, $q = \epsilon_y^2 (\epsilon_x - n_z^2)(\epsilon_x - \epsilon_z)$ and $r = \epsilon_y^2 (n_z^2 - \epsilon_x + \epsilon_z)$ with a similar expression for δ_2. For the MHD limit $\omega \to 0$, $\epsilon_y \to 0$ and $\delta_1 = \delta_2 \equiv 0$, so that (5) and (6) exhibit purely compressional and torsional character respectively. Barring the extremely weak contributions from the collisional and cyclotron damping terms in (2), the CAW is essentially undamped. The KAW, on the contrary, is efficiently absorbed by ELD with a damping length

$$k_{xi}^{-1} \simeq \frac{1}{(2\pi)^{1/2}} \frac{\omega}{\omega_{pe}} \frac{\exp(-\zeta_e^2)}{\zeta_e^2} , \tag{8}$$

which is typically only a few centimeters for $\zeta_e \sim O(.1)$ and is not much affected by finite values of k_y. Non-zero k_y introduces a weak ELD in CAW through the correction term δ_1 in (5). The damping length

$$k_{xi}^{-1} \simeq \frac{\beta}{\sqrt{\pi}} \frac{c}{\omega} \left(\frac{\omega_{pe}}{\omega}\right)^2 \left(\frac{\omega_{ci}}{\omega}\right)^2 \left(\frac{\omega_{ci}}{\omega_{pi}}\right)^4 \epsilon_x^{1/2} \zeta_e \exp(\zeta^2) , \tag{9}$$

is typically well over 10^{10} cm. This damping is even weaker than the collisional absorption. If instead of ELD, v_p is picked to be in the vicinity of v_{zi} to facilitate ion Landau damping, k_x^{-1} in (9) is decreased by (M/m) and ζ_i^{-3} replaces ζ_e. In this case k_{xi}^{-1} is typically over 10^{15} cm implying a very weak absorption. The combined collisional and electron or ion Landau damping appears to be too weak to allow effective plasma heating through the mechanism of transit time magnetic pumping.

From the Maxwell's equations one may readily confirm that the two waves exist independently of each other[7] and no coupling from CAW to KAW is possible in case $k_y = 0$. For finite ω, k_y is non-zero and a coupling between the two waves becomes, in principle, possible. The remainder of this paper is devoted to the quantitative determination of the extent of this coupling.

Although, the Maxwell's equations may be reduced to a single fourth order differential equation, the resultant equation is mathematically intractable with the existing techniques. Also the plasma parameters vary too rapidly to allow WKB analysis, leaving numerical methods as the only remaining choice. Following much trial and travail, the most suitable numerical technique was a combination of an integration of the set of the four first-order Maxwell's equations from $x_\kappa = x_{c1} - |\kappa|$ to $x = 0$, where κ is an arbitrary and uncritical choice. Between $x = -a$ and x_κ, numerical integration becomes unstable due to the strong evanescence of the KAW. Instead a stepped slab plasma model[8] with 85 plasma steps has been used. This has the advantage of retaining machine accuracy in the solution, there being no exponential buildup of numerical errors because of the simultaneous boundary conditions, requiring the continuity of the tangential electric and magnetic fields, to be satisfied between adjacent plasma steps. Also, negligible error is introduced by assuming a stepped, constant density profile between adjacent sheets because the sheet separation is small compared to the evenescence length of the CAW while any inaccuracies in KAW are easily tolerated without significant bearing on the results because this wave is, in any case, conspicuous by its absence in this region.

For the plasma and field parameters of Table 1 and using the boundary condition that at $x = 0$ both CAW and KAW propagate away from the antenna,

the Poynting flux entering the plasma surface at x = -a is $P_{x=-a} = 0.658\ W/m^2$. This compares favorably with the resistive dissipation of a steel antenna of about 1 mW/m^2 with a corresponding quality factor Q = 0.2. A closer examination reveals, however, that the Poynting vector continues undiminished past x_A indicating a poor coupling to the KAW. This is confirmed by placing a second antenna at x = b with the plasma density profile symmetric around x = 0 . Depending upon the symmetric or antisymmetric excitation of the two antennae, the Poynting vector flux into the plasma is 56 μW and 0.13 μW respectively. The corresponding Q values are 1.5×10^3 and 1.8×10^6 while the heating efficiencies are below 1 % and 0.01 % respectively.

These results are only marginally affected by variations in plasma temperature, profile, position of the Alfvèn surface or by incorporating collisional damping. The best heating occurs for low density gradients because of the increased interaction region for wave conversion and for small plasma widths (and antenna separation from the plasma) because of the weaker evanescence of CAW between the antenna and the wave conversion region. Even at its best, the heating efficiency remains below 10 %.

A further source of coupling between CAW and KAW, not taken into account in this paper, is a non-zero k_y. We propose to present the effect of including k_y, effect of magnetic field and temperature gradients along with a comparison of our results with the MHD theory as well as details of the numerical techniques in an expanded version of this communication. An attempt will be made to seek comparison of the theory with the existing experimental results.

Regarding the computational reliability of the results presented here, no particular difficulteis were encountered in either the integration of the Maxwell's equations or in solving the 4x85 simultaneous complex equations of the stepped slab geometry since the entire region $-a \leq x \leq 0$

is free of singularities. This is unlike the case of the MHD treatment in which the KAW becomes singular at x_A because of the neglect of electron inertia with a simultaneous coalescence of x_{c1} and x_{c2} with X_A through assuming that $\omega \to 0$. In the critical region surrounding X_A the integration was performed with a relative numerical tolerance of one part in 10^{12} using a sixth order Runge-Kutta procedure. Reversing the integration reproduces the starting values to one part in 10^6. The 4x85 complex simultaneous equations were solved with a quadruple accuracy Gauss elimination procedure followed by iterative refinement to machine accuracy. A further check made on the continuity of the Poynting vector at each slab boundary revealed an accuracy better than one part in 10^6.

REFERENCES

1 J.A. Tataronis and W. Grossman, Z. Phys. 261, 217 (1973).

2 A. Hasegawa and L. Chen, Phys. Rev. Lett. 32, 454 (1974); Phys. Fluids 17, 1399 (1974).

3 A. Hasegawa and L. Chen, Phys. Rev. Lett. 35, 370 (1975).

4 A. Hasegawa, Phys. Fluids 19, 1924 (1976).

5 T.H. Stix, Proceedings of the Symposium on Heating in Toroidal Plasmas, Grenoble, Vol. II, 363 (1978); Bull. APS 23, 863 (1978).

6 B.D. Fried and S.D. Conte, The Plasma Dispersion Function, (Academic, New York, 1961).

7 S. Puri and J.A. Tataronis, Bull. APS 23, 863 (1978); Max-Planck IPP Report IPP 4/173, 8046 Garching (1978).

8 S. Puri and M. Tutter, Nucl. Fusion 14, 93 (1974).

FIGURE AND TABLE CAPTIONS

Fig. 1 Geometry of the model employed.

Fig. 2 k_x^2 versus density for both the CAW (k_{xc}^2) and the KAW (k_{xK}^2). The dashed line shows the imaginary part of k_{xK}^2.

Table 1 Plasma and field parameters used in the computations.

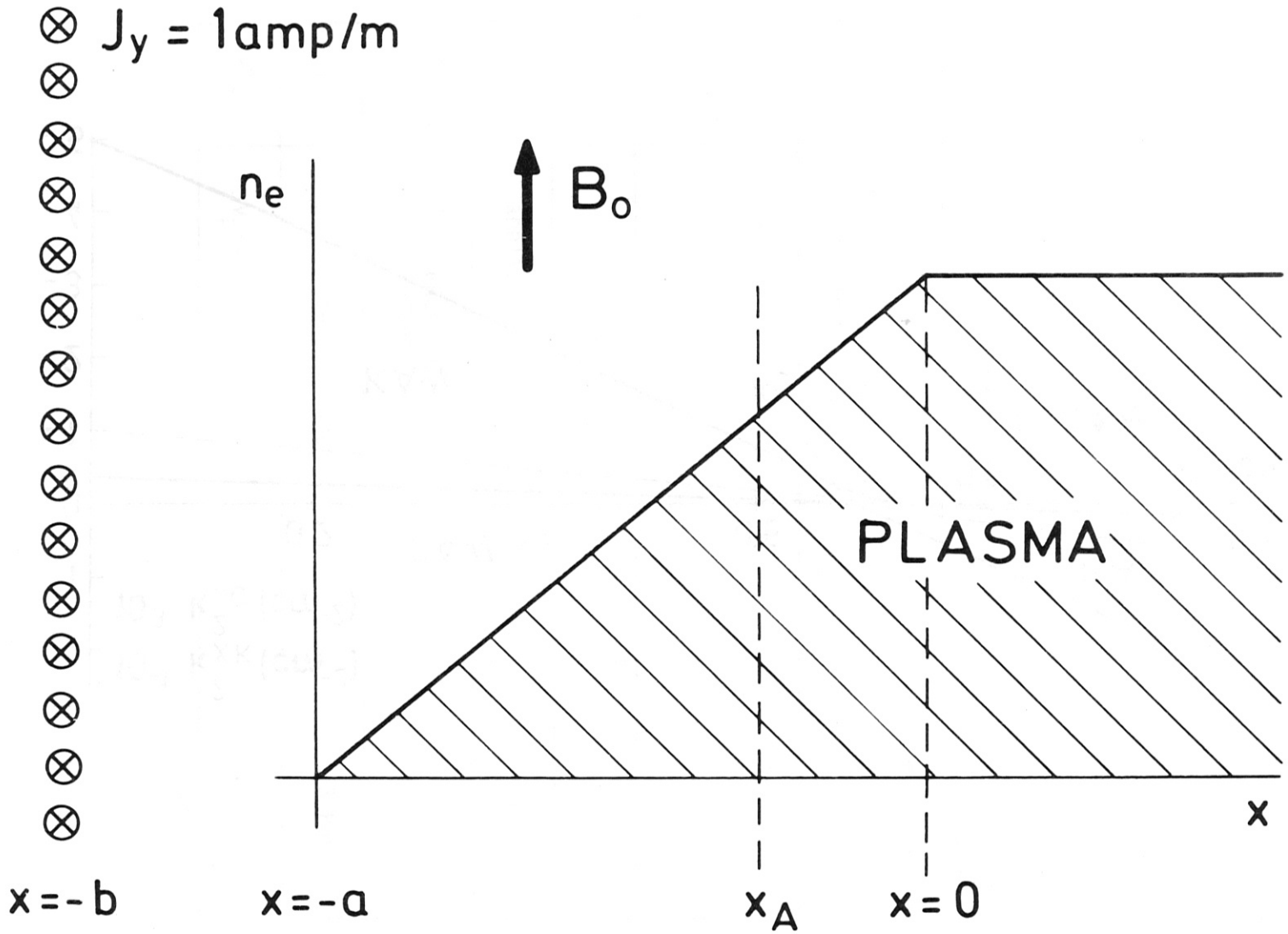
J_y = 1amp/m
n_e
B_o
PLASMA
x
x=-b
x=-a
x_A
x=0

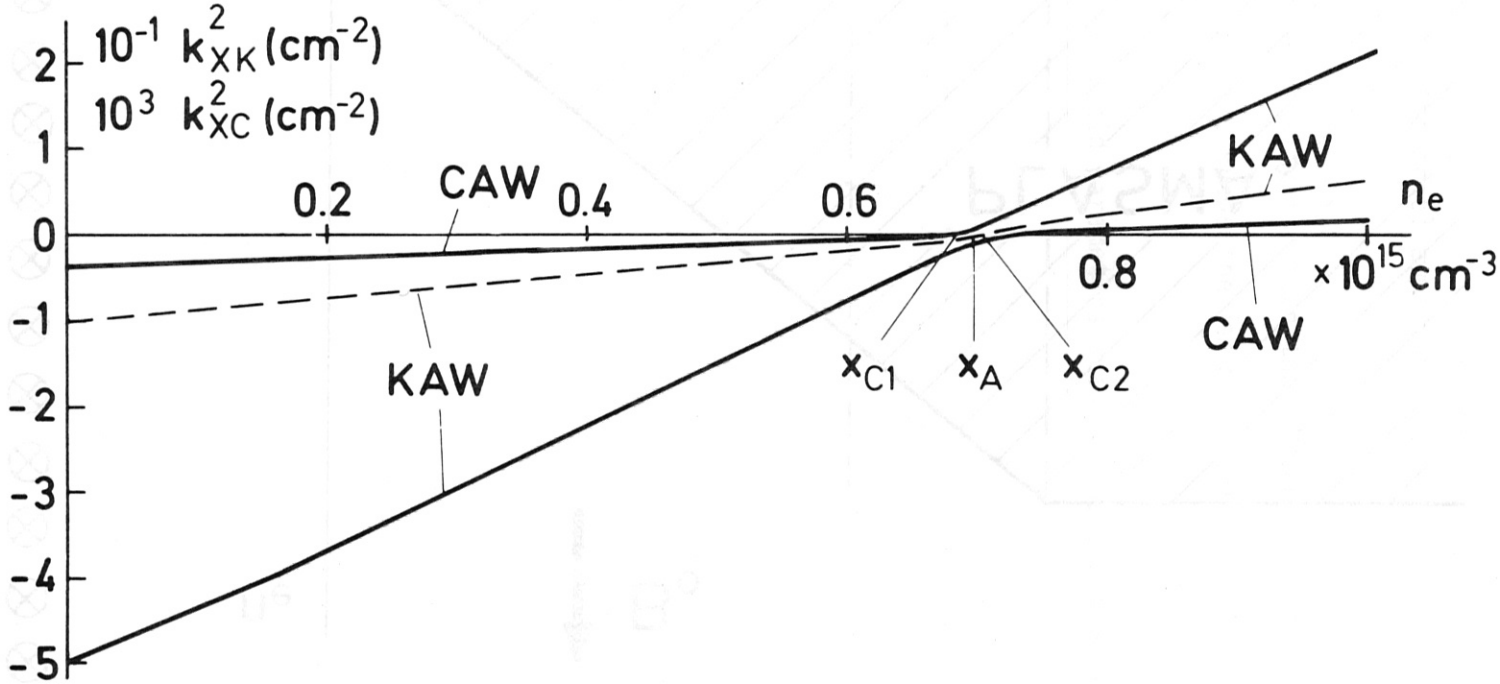
$10^{-1}\ k^2_{XK}\ (cm^{-2})$
$10^{3}\ k^2_{XC}\ (cm^{-2})$
2
1
0
-1
-2
-3
-4
-5
0.2
0.4
0.6
0.8
CAW
KAW
KAW
CAW
n_e
$\times 10^{15} cm^{-3}$
x_{C1}
x_A
x_{C2}

Table 1

B_o	static magnetic field	60 kG
n_{max}	maximum electron density	10^{15} cm^{-3}
λ_z	parallel wavelength	10 m
a	plasma profile length	30 cm
b	antenna position	40 cm
X_A	position of Alfvèn surface from plasma edge	21 cm
x_{c1}	position of the left cutoff	20.8 cm
x_{c2}	position of the right cutoff	21.2 cm
n_z	parallel refractive index	96
f	applied frequency	3.1×10^5 Hz
f/f_{CD}	frequency relative to deuterium gyrofrequency	.007
T	plasma temperature	3 keV
ζ_e	v_p/v_{ze}	.104